

Manganese and Rhenium Metalloboranes Containing Tridentate Borane Ligands $B_9H_{13}^{2-}$ and $B_9H_{12}L^-$ ($L =$ Tetrahydrofuran or Diethyl Ether)

J. W. LOTT and D. F. GAINES*

Received February 26, 1974

AIC40130V

A new class of metalloboranes which is structurally similar to $B_{10}H_{14}$ has been characterized. These new metalloboranes contain tridentate B_9 ligands bound to the metal by two M-H-B bridge hydrogen bonds and a M-B σ -bond interaction. They are prepared by reactions of KB_9H_{14} with $Mn(CO)_5Br$ and $Re(CO)_5Br$ in ethereal solvents under a variety of conditions. The following metalloboranes have been characterized: 2-THF-6-(CO) $_3$ -6-MnB $_9$ H $_{12}$, 5-THF-6-(CO) $_3$ -6-MnB $_9$ H $_{12}$, 2-Et $_2$ O-6-(CO) $_3$ -6-MnB $_9$ H $_{12}$, and salts of 6-(CO) $_3$ -6-MnB $_9$ H $_{13}^-$ and 6-(CO) $_3$ -6-ReB $_9$ H $_{13}^-$. The X-ray crystal structure of 5-THF-6-(CO) $_3$ -6-MnB $_9$ H $_{12}$ was solved by conventional heavy-atom techniques and has been refined to $R_1 = 0.045$ and $R_2 = 0.055$ for 1803 reflections measured on a Syntex PI autodiffractometer. The crystals are in the triclinic space group $P\bar{1}$ and the unit cell dimensions are $a = 9.828$ (3) Å, $b = 13.305$ (5) Å, $c = 6.937$ (2) Å, $\alpha = 90.1$ (2) $^\circ$, $\beta = 104.23$ (2) $^\circ$, $\gamma = 109.87$ (3) $^\circ$, $V = 822.1$ (5) Å 3 , and $Z = 2$.

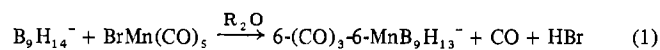
Introduction

Metalloboranes of the type to be considered here consist of a borane polyhedral fragment in which one boron position is occupied by a metal. In most cases reported prior to 1973 the borane portions of metalloboranes have been considered formally to be bidentate ligands bonded to the metal by two equivalent bonding interactions.¹ For example, in $[(CO)_4CrB_3H_8]^-$ the $B_3H_8^-$ ligand is bound to Cr by two equivalent Cr-H-B bridge hydrogen bonds from two adjacent boron atoms.² In the case of $[Ni(B_{10}H_{12})_2]^{2-}$ the $B_{10}H_{12}^{2-}$ ligand is considered to be bidentate, and the X-ray determined molecular symmetry requires that both bonding interactions to the metal be identical.³

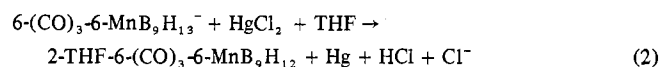
Presented here are examples of a new class of metalloboranes in which the borane ligand $B_9H_{13}^{2-}$ and derivatives thereof are tridentate and bound to the metal by two different types of bonding interaction.

Results and Discussion

This report is concerned with the characterization of the major products of the reaction of the group VIIIb metal pentacarbonyl halides $Mn(CO)_5Br$ and $Re(CO)_5Br$ with the salts of the tetradecahydroborate(1-) anion, $B_9H_{14}^-$, in ethereal solvents. The types and quantities of the several products of this reaction depend primarily on the ratio of the reactants and the choice of ether solvent. When equimolar quantities of $Mn(CO)_5Br$ and KB_9H_{14} are heated to reflux in tetrahydrofuran (THF), carbon monoxide is evolved and the solution turns red. The major reaction product subsequently isolated is the tetramethylammonium salt of 6-(CO) $_3$ -6-MnB $_9$ H $_{13}^-$, I, along with smaller amounts of 2-THF-6-(CO) $_3$ -6-MnB $_9$ H $_{12}$, II. The idealized major reaction is shown in eq 1. The small



amounts of II isolated from the reaction are undoubtedly a result of the formation of an unidentified oxidizing agent in a side reaction. Separate experiments have shown that I may be oxidized to II in THF using I_2 or $HgCl_2$ as represented by the idealized reaction in eq 2.



(1) For a review see E. L. Muetterties, *Pure Appl. Chem.*, **29**, 585 (1972).

(2) L. J. Guggenberger, *Inorg. Chem.*, **9**, 367 (1970).

(3) L. J. Guggenberger, *J. Amer. Chem. Soc.*, **94**, 114 (1972).

Two equivalents of $Mn(CO)_5Br$ reacts with KB_9H_{14} in refluxing THF to produce, in addition to I and II, a structural isomer of II, which has been found to be 5-THF-6-(CO) $_3$ -6-MnB $_9$ H $_{12}$, III.

The reaction of equimolar quantities of $Mn(CO)_5Br$ and KB_9H_{14} in refluxing diethyl ether (Et $_2$ O) produces primarily I, along with 2-Et $_2$ O-6-(CO) $_3$ -6-MnB $_9$ H $_{12}$, IV, the ether analog of II, and a new boron elision product (CO) $_3$ MnB $_8$ H $_{13}$, which will be discussed in a future publication.

Substitution of $Re(CO)_5Br$ for $Mn(CO)_5Br$ in the reaction with KB_9H_{14} in refluxing THF produced the rhenium analog of I, which was subsequently isolated as the tetramethylammonium salt of 6-(CO) $_3$ -6-ReB $_9$ H $_{13}^-$, V. An unstable species that appeared to be the rhenium analog of II was also isolated, but it has not been fully characterized.

The metalloboranes I-IV are all red-orange crystalline materials that do not noticeably decompose in air. They do not appear to be readily hydrolyzed in aqueous solution and the ionic complexes are crystallized from aqueous solutions. These complexes are less stable in organic solvents, as evidenced by the slow formation of white precipitates in these solutions. The rate of decomposition appears to decrease as the purity of the complex increases.

The structural similarities of the metalloborane frameworks of I, II, IV, and V were clearly indicated by their spectroscopic properties. Novel bonding interactions between the borane ligand and manganese (or rhenium) were suggested on the basis of preliminary studies of physical properties and spectroscopic characteristics. The complexity of these metalloboranes was great enough, however, to preclude unequivocal structural assignments. Thus several single-crystal X-ray studies have been undertaken in order to establish the structural characteristics of this class of metalloboranes. The structure of II, shown in Figure 1, illustrates their general structural features.⁴ The symmetry of II is C_3 and the symmetry plane passes through Mn, B $_2$, O $_4$, B $_4$, and B $_9$. Spectroscopic evidence indicates that I, IV, and V undoubtedly contain a similar symmetry plane. Other related metalloboranes that do not contain a symmetry plane have subsequently been prepared. The physical properties of these asymmetric metalloboranes were not significantly different from those of I, II, IV, and V. Their spectroscopic properties, however, especially their ^{11}B and 1H nmr spectra, were very complex compared to those of their more symmetric relatives,

(4) R. Schaeffer, H. Shenhav, J. W. Lott, and D. F. Gaines, *J. Amer. Chem. Soc.*, **95**, 3042 (1973).

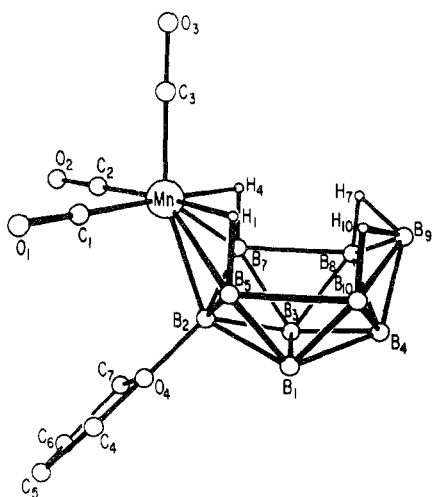


Figure 1. The structure of 2-THF-6-(CO)₃-6-MnB₉H₁₂, II. For clarity the terminal hydrogens have been omitted from the coordinate THF and from B₁, B₃-B₅, and B₇-B₁₀.

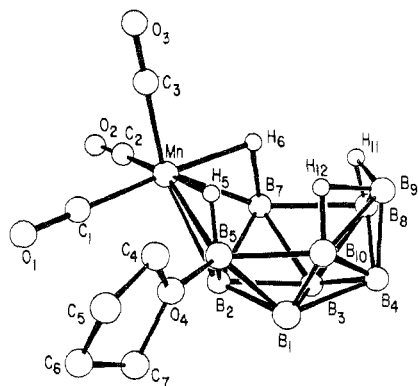


Figure 2. The structure of 5-THF-6-(CO)₃-6-MnB₉H₁₂, III. Terminal hydrogens have been omitted from the THF and B₁-B₄ and B₇-B₁₀.

and the data appeared intractable at that time. For this reason an X-ray crystallographic study of III, a structural isomer of II, was initiated.

The structure of III (less terminal hydrogen atoms) is shown in Figure 2. Interatomic distances and angles are shown in Tables I and II, respectively. The unit cell of crystalline III (space group *PI*) contains a centrosymmetrically related *dl* pair of 5-THF- and 7-THF-6-(CO)₃-6-MnB₉H₁₂ molecules, and references to the B(5)-substituted isomer apply to the equivalent B(7)-substituted isomer. In the structure of III and in the previously reported structure of 8-(Et₃N(CH₂)₄O)-6-(CO)₃-6-MnB₉H₁₂,⁵ a lengthening of 0.04–0.05 Å is seen in the B(5)–B(10) distance (the side of the molecule bearing the substituent) compared to the corresponding B(7)–B(8) distance. In the more symmetric II, the B(7)–B(8) and B(5)–B(10) distances are virtually identical. This distortion of some bond distances in the upper tier of boron atoms in III is not complemented by any significant distortion of B–B distances in the lower part of the cage and in fact the B(1)–B(2) distances are 1.776 (3) Å for all three compounds noted above. The quasi-octahedral environment of the manganese also appears to be independent of the point of substitution on the borane cage. Here as in the cases mentioned above, the Mn–B distances to B(2), B(5), and B(7) are very nearly the same

Table I. Interatomic Distances (Å) for 5-THF-6-(CO)₃-6-MnB₉H₁₂, III

Mn–C(1)	1.796 (5)	B(4)–B(8)	1.779 (7)
C(2)	1.797 (5)	B(9)	1.711 (8)
C(3)	1.814 (5)	B(10)	1.782 (7)
B(2)	2.226 (4)	H(4)	1.04
B(7)	2.206 (5)	B(5)–B(10)	1.993 (6)
B(5)	2.232 (4)	O(4)	1.520 (5)
H(6) _B	1.83	H(5) _B	1.26
H(5) _B	1.67	B(7)–B(8)	2.037 (7)
B(1)–B(2)	1.774 (6)	H(6) _B	1.27
B(3)	1.775 (6)	H(7)	1.18
B(4)	1.784 (7)	B(8)–B(9)	1.774 (7)
B(5)	1.733 (6)	H(8)	1.15
B(10)	1.750 (7)	H(11) _B	1.19
H(1)	1.12	B(9)–B(10)	1.781 (7)
B(2)–B(3)	1.774 (6)	H(9)	1.12
B(7)	1.807 (6)	H(11) _B	1.19
B(5)	1.764 (6)	H(12) _B	1.36
H(2)	1.11	B(10)–H(10)	1.12
B(3)–B(4)	1.803 (7)	H(12) _B	1.17
B(7)	1.770 (7)		
B(8)	1.758 (7)		
H(3)	1.19		
		Tetrahydrofuran Molecule	
C(4)–O(4)	1.478 (5)	C(6)–C(7)	1.524 (7)
C(5)	1.483 (6)	H(17)	0.87
H(13)	0.88	H(18)	0.72
H(14)	0.87	C(7)–O(4)	1.480 (5)
C(5)–C(6)	1.486 (8)	H(19)	0.74
H(15)	1.25	H(20)	0.87
H(16)	0.85		
		Carbonyl Distances	
C(1)–O(1)	1.146 (5)	C(3)–O(3)	1.143 (5)
C(2)–O(2)	1.150 (5)		

(2.22 (2) Å). All other distances are comparable for the three compounds.

An interesting feature of these two THF-substituted compounds, II and III, is the lack of planarity of the THF ring. A structure was recently described by Hodgson and Raymond in which two THF molecules were present, one in each of the two predominant conformations, the skew or twist conformation (*C₂*) and the envelope conformation (*C_s*).⁶ Using a program to calculate the best least-squares planes, perpendicular distances to these planes, and angles between planes,⁷ it was found that the THF in II has an envelope conformation with a dihedral angle of 7.6°, while in III the THF has a twist conformation. The angle between the THF ring and the B(5)–B(7)–B(8)–B(10) plane in III is 116.79° (see Table III).

Nmr Discussion. The nmr spectra of the B₉ metalloboranes can be interpreted with considerable confidence in light of the X-ray structural data and the gross similarities of some spectral regions to those of the structural analog B₁₀H₁₄. The B₉ metalloborane structures are derived from that of B₁₀H₁₄ by replacing the B(6)–H group with a M(CO)₃ group. The ¹¹B spectrum of B₁₀H₁₄ consists of three groups of resonances. The two pairs B(1), B(3) and B(6), B(9) resonate at lowest field. The midfield resonance arises from the four equivalent borons B(5), B(7), B(8), and B(10), while the highest field resonance arises from the equivalent B(2), B(4) pair.⁸ When the B₁₀H₁₄ cage is altered by replacing the

(6) K. O. Hodgson and K. N. Raymond, *Inorg. Chem.*, 11, 171 (1972).

(7) D. L. Smith, Ph.D. Thesis (Appendix), University of Wisconsin, Madison, Wis., 1962.

(8) G. R. Eaton and W. N. Lipscomb, "NMR Studies of Boron Hydrides and Related Compounds," W. A. Benjamin, New York, N. Y., 1969.

(5) D. F. Gaines, J. W. Lott, and J. C. Calabrese, *J. Chem. Soc., Chem. Commun.*, 295 (1973).

Table II. Bond Angles (deg)^a for 5-THF-6-(CO)₃-6-MnB₉H₁₂, III

C(3)-Mn-H(5)	90.60	C(1)-Mn-C(2)	88.46 (21)
C(3)-Mn-H(6)	91.73	C(2)-Mn-C(3)	92.61 (19)
C(1)-Mn-H(5)	96.09	C(2)-Mn-B(2)	101.86 (18)
C(1)-Mn-H(6)	173.53	C(2)-Mn-B(7)	82.27 (19)
C(2)-Mn-H(5)	174.28	C(2)-Mn-B(5)	147.24 (18)
C(2)-Mn-H(6)	87.15	C(3)-Mn-B(7)	126.46 (18)
B(2)-Mn-H(5)	74.25	C(1)-Mn-C(3)	93.22 (20)
B(2)-Mn-H(6)	79.91	C(1)-Mn-B(7)	139.42 (19)
B(7)-Mn-H(5)	92.91	C(1)-Mn-B(5)	87.11 (17)
B(7)-Mn-H(6)	35.03	C(1)-Mn-B(2)	96.36 (18)
B(5)-Mn-H(5)	30.31	C(3)-Mn-B(2)	162.82 (17)
B(5)-Mn-H(6)	94.01	C(3)-Mn-B(5)	120.04 (17)
B(2)-Mn-B(7)	48.13 (16)	B(1)-B(2)-B(7)	106.77 (30)
B(2)-Mn-B(5)	46.62 (15)	B(1)-B(2)-B(5)	58.65 (24)
B(7)-Mn-B(5)	80.22 (16)	B(7)-B(2)-B(5)	106.33 (29)
Mn-C(1)-O(1)	176.15 (44)	B(10)-B(1)-B(5)	69.83 (27)
Mn-C(2)-O(2)	177.18 (40)	B(10)-B(1)-B(3)	107.73 (32)
Mn-C(3)-O(3)	179.22 (39)	B(10)-B(1)-B(4)	60.57 (27)
B(2)-B(3)-B(1)	60.00 (24)	B(10)-B(1)-B(2)	117.70 (33)
B(7)-B(3)-B(8)	70.56 (29)	B(3)-B(1)-B(2)	59.91 (25)
B(2)-B(3)-B(4)	114.16 (32)	B(3)-B(1)-B(4)	60.89 (27)
B(2)-B(3)-B(7)	61.37 (26)	B(3)-B(1)-B(5)	107.67 (31)
B(2)-B(3)-B(8)	118.85 (33)	B(2)-B(1)-B(4)	115.07 (33)
B(1)-B(3)-B(4)	59.79 (26)	B(2)-B(1)-B(5)	60.41 (24)
B(1)-B(3)-B(7)	108.35 (31)	B(4)-B(1)-B(5)	118.77 (34)
B(1)-B(3)-B(8)	107.14 (32)	B(9)-B(4)-B(8)	61.07 (30)
B(4)-B(3)-B(7)	118.44 (34)	B(3)-B(4)-B(1)	59.33 (25)
B(4)-B(3)-B(8)	59.93 (28)	B(3)-B(4)-B(10)	105.13 (32)
B(7)-B(2)-B(1)	106.77 (30)	B(3)-B(4)-B(9)	110.26 (37)
B(3)-B(2)-B(1)	60.10 (25)	B(3)-B(4)-B(8)	58.76 (28)
B(3)-B(2)-B(7)	59.25 (26)	B(1)-B(4)-B(10)	58.77 (26)
B(3)-B(2)-B(5)	106.43 (30)	B(1)-B(4)-B(9)	110.81 (35)
Mn-B(2)-B(3)	119.19 (26)	B(10)-B(4)-B(8)	105.07 (35)
Mn-B(2)-B(1)	119.77 (26)	B(8)-B(7)-H(5)	90.80
Mn-B(2)-B(7)	65.33 (20)	B(8)-B(7)-H(6)	87.88
Mn-B(2)-B(5)	66.84 (20)	B(9)-B(10)-B(8)	37.25 (21)
B(8)-B(7)-B(2)	104.29 (30)	B(4)-B(10)-B(9)	57.39 (29)
B(8)-B(7)-B(5)	88.93 (22)	B(4)-B(9)-B(10)	61.33 (29)
B(8)-B(7)-B(3)	54.44 (25)	B(4)-B(9)-B(8)	61.36 (30)
Mn-B(7)-B(8)	124.59 (26)	B(10)-B(9)-B(8)	105.32 (34)
Mn-B(7)-B(3)	120.39 (27)	B(3)-B(8)-B(4)	61.31 (28)
Mn-B(7)-B(2)	66.54 (20)	B(7)-B(8)-B(10)	90.17 (22)
B(3)-B(7)-B(2)	59.38 (25)	B(9)-B(8)-B(7)	116.56 (32)
B(10)-B(5)-H(5)	92.85	B(9)-B(8)-B(3)	109.48 (34)
B(10)-B(5)-H(6)	88.62	B(9)-B(8)-B(10)	37.43 (21)
B(10)-B(5)-Mn	124.10 (25)	B(4)-B(8)-B(9)	57.57 (31)
B(10)-B(5)-B(7)	90.15 (22)	O(4)-B(5)-B(10)	111.20 (29)
B(10)-B(5)-B(2)	106.59 (28)	Mn-B(5)-O(4)	117.04 (25)
B(10)-B(5)-B(1)	55.49 (24)	B(5)-O(4)-C(4)	122.78 (28)
Mn-B(5)-B(2)	66.53 (20)	B(5)-O(4)-C(7)	125.14 (31)
Mn-B(5)-B(1)	121.51 (26)	O(4)-C(4)-C(5)	104.76 (36)
B(2)-B(5)-B(1)	60.95 (24)	C(4)-C(5)-C(6)	108.33 (40)
B(1)-B(10)-B(4)	60.66 (27)	C(5)-C(6)-C(7)	106.63 (42)
B(5)-B(10)-B(8)	90.72 (23)	C(6)-C(7)-C(4)	102.58 (40)
B(5)-B(10)-B(4)	106.43 (31)	Mn-H(5)-B(7)	51.59
B(5)-B(10)-B(1)	54.68 (23)	Mn-H(5)-B(5)	102.82
B(9)-B(10)-B(5)	117.66 (33)	Mn-H(6)-B(7)	88.95
B(9)-B(10)-B(1)	109.13 (33)	Mn-H(6)-B(5)	48.27
B(1)-B(4)-B(8)	105.86 (33)		
B(10)-B(4)-B(9)	61.28 (30)		

^a Standard deviations are in parentheses.

B(6)-H group with a M(CO)₃ group, the boron atoms closest to the metal are expected to have their chemical shifts modified the most. By examination of Table IV it can be seen that the ¹¹B nmr spectrum of I shows the spectral changes expected—namely, that the B(2) resonance is different from the B(4) resonance and the B(5), B(7) resonance is different from the B(8), B(10) resonance. The ¹¹B nmr spectrum of II is shown in Figure 3, along with the resonance assignments. As is indicated, substitution of a Lewis base for H⁻ on B(2) causes a large downfield shift of that resonance. It is interesting to note that MHB bridge hydrogen coupling is resolved on the B(5), B(7) resonances (as it is in the ¹H nmr spectrum), but the BHB bridge hydrogen coupling to B(8), B(9), and

Table III. Equations of Best Least-Squares Planes, Distances of Selected Atoms from These Planes, and Dihedral Angles between These Planes^a in 5-THF-6-(CO)₃-6-MnB₉H₁₂, III

(a) Plane through O(4), C(4), C(5), C(6), and C(7)			
0.618X + 0.708Y - 0.342Z - 3.419 = 0			
O(4)	-0.07	C(6)	-0.14
C(4)	-0.02	C(7)	0.12
C(5)	0.10		
(b) Plane through B(5), B(7), B(8), and B(10)			
-0.063X - 0.841Y - 0.537Z - 3.718 = 0			
B(5)	0.01	B(8)	0.01
B(7)	-0.01	B(10)	-0.01
(c) Plane through O(4), C(4), and C(7)			
0.731X + 0.604Y - 0.318Z - 3.082 = 0			
C(5)	-0.10	B(5)	0.05
C(6)	-0.44		
(d) Plane through C(4), C(5), C(6), and C(7)			
0.577X - 0.730Y - 0.367Z - 3.535 = 0			
C(4)	-0.08	C(7)	0.07
C(5)	0.13	O(4)	-0.16
C(6)	-0.12		
B. Dihedral Angles (deg) between Normals to Planes			
a-b	116.8	b-c	112.5
c-d	11.8	b-d	117.0

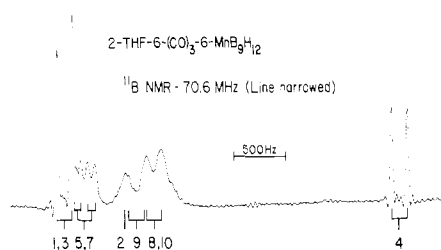
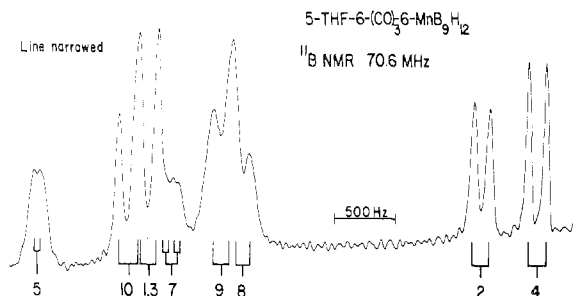
^a Unit weights were used for all atoms in the application of the Smith least-squares planes program modified by J. C. Calabrese.⁷

Table IV. ¹¹B Nmr Data

Compd	Chem shift ^a	Assignments ^b
B ₁₀ H ₁₄	-11.3	1, 3
	-9.7	6, 9
	-0.7	5, 7, 8, 10
	35.8	24
I, ^c [Me ₄ N] ⁺ [6-(CO) ₃ -6-MnB ₉ H ₁₃] ⁻	-10.8	1, 3
	-9.2 ^d	5, 7
	-0.1	9
	1.8	8, 10
II, ^c 2-THF-6-(CO) ₃ -6-MnB ₉ H ₁₂	27.6	2
	34.3	4
	-8.9	1, 3
	-6.1 ^d	5, 7
	-0.4 s ^e	2
	1.1	9
III, ^c 5-THF-6-(CO) ₃ -6-MnB ₉ H ₁₂	3.3	8, 10
	36.5	4
	-21.7 s ^d	5
	-10.8	1, 3
	-8.5	10
	-6.2	7
	0.3	9
	2.4	8
IV, 2-Et ₂ O-6-(CO) ₃ -6-MnB ₉ H ₁₂	31.2	2
	37.8	4
	-9.6	(1, 3, 2) ^f
	-34	(5, 7, 9) ^f
	4.2	(8, 10) ^f
	37.4	4
V, [Me ₄ N] ⁺ [6-(CO) ₃ -6-ReB ₉ H ₁₃] ⁻	-7.5	(1, 3, 5, 7) ^f
	0.9	(9, 8, 10) ^f
	31.2	2
	38.2	4

^a Chemical shifts in ppm from BF₃·OEt₂ standard. All unlabeled shifts correspond to doublets with ¹¹B-H coupling constants in the range 140-160 Hz. ^b The numbering system used is shown in Figures 1 and 2. ^c This spectrum was obtained at 32.1 and 70.6 MHz. Others were obtained at 32.1 MHz only. ^d Bridge hydrogen couplings of ~70 Hz are observed in the 70.6-MHz line-narrowed spectra. ^e The symbol "s" designates a singlet resonance. ^f Assignments in parentheses are tentative.

B(10) is apparently much smaller and is not resolved in B₁₀H₁₄ or in any of the presently known metalloboranes. The ¹¹B nmr spectrum of III, shown in Figure 4, illustrates the spectral

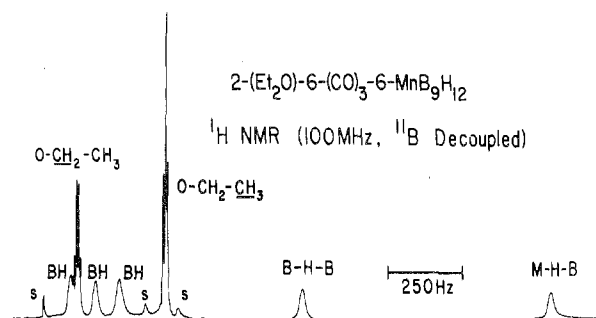
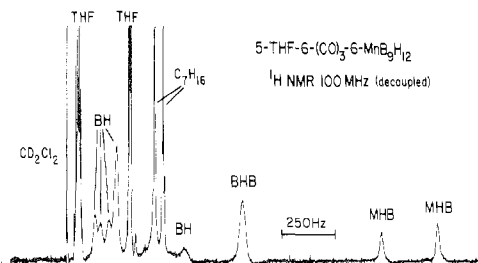
Figure 3. The ^{11}B nmr spectrum of 2-THF-6-(CO) $_3$ -6-MnB $_9$ H $_{12}$, II.Figure 4. The ^{11}B nmr spectrum of 5-THF-6-(CO) $_3$ -6-MnB $_9$ H $_{12}$, III.

changes that occur when the symmetry plane of the B $_9$ metalloboranes is removed. The spectrum contains two upfield doublets corresponding to B(2) and B(4). The B(5) resonance, which is substituted with THF, is shifted downfield to the lowest position. Along with the downfield shift in B(5) there is an apparent downfield shift of the B(10) resonance. A suggestion of MnHB bridge hydrogen coupling is indicated on the B(5) and B(7) resonances. The 32.1-MHz ^{11}B nmr spectrum of IV is very similar to that of II. Likewise, the spectrum of VI is similar in appearance to that of I, except that the lower field resonances from I cover a larger chemical shift range than the low-field resonances of VI and the intensities of the two low-field doublets are reversed (in I the lowest field doublet is the strongest).

The ^1H nmr spectra of the B $_9$ metalloboranes are tabulated in Table V. The most important features of these spectra are the characteristic resonances arising from MHB and BHB bridge hydrogens. The MHB hydrogens occur at $\tau \sim 18$ -21, a shift region characteristic of metal hydride type hydrogens. The BHB hydrogens occur at $\tau \sim 12$ -14 and are easily distinguished from terminal BH resonances because of their much smaller coupling interactions with ^{11}B . Figure 5 shows the ^1H nmr spectrum of IV obtained with ^{11}B decoupled. The ethyl resonances of the ether ligand are readily identified, and a mirror plane in the complex is indicated by the appearance of a single type of BHB hydrogens and an equal number of a single type of MHB hydrogens. Figure 6 shows the ^1H nmr spectrum of III. The lower symmetry of III, compared to that of IV, is indicated by the presence of two types of MHB hydrogens and several more distinct types of BH terminal hydrogens. The two BHB hydrogens, however, do not appear to be very sensitive to this remote loss of symmetry. The heptane in the spectrum of III is occluded recrystallization solvent.

The mass spectra of the slightly volatile II, III, and IV all exhibit parent m/e envelopes corresponding to the calculated isotopic mixtures. The most intense fragments obtained correspond to the parent minus three CO ligands, $P - 3(\text{CO})$, then $P - (\text{CO}) - \text{L}$, followed by P , and $P - 2(\text{CO})$. In no case was a significant $P - (\text{CO})$ fragment observed. It is interesting⁹ to note that significant hydrogen loss does not become

(9) J. F. Ditter, F. J. Gerhart, and R. E. Williams, *Advan. Chem. Ser.*, No. 72, 191 (1968).

Figure 5. The ^1H nmr spectrum of 2-Et $_2$ O-6-(CO) $_3$ -6-MnB $_9$ H $_{12}$, IV, with ^{11}B decoupled.Figure 6. The ^1H nmr spectrum of 5-THF-6-(CO) $_3$ -6-MnB $_9$ H $_{12}$, III, with ^{11}B decoupled. The C $_7$ H $_{16}$ impurity is occluded recrystallization solvent.Table V. ^1H Nmr Data^a (τ)

Compd ^b	B-H terminal	B-H-B bridge	M-H-B bridge ^c	Other ^d
I	6.2	13.0	21.4	7.0 (Me $_4$ N $^+$)
	6.7			
	7.3			
	9.5			
	10.8			
II	6.0	13.7	21.9	6.4 (THF) 8.4 (THF)
	6.9			
	7.7			
	9.2			
	9.6			
III	6.0	12.7	19.2	5.2 (THF) 7.6 (THF)
	6.2			
	6.6			
	7.0			
	10.1			
IV	5.6	13.3	21.6	5.8 (Et $_2$ O) 8.7 (Et $_2$ O)
	6.4			
	7.2			
V	5.9	13.3	18.0	6.9 (Me $_4$ N $^+$)
	6.1			
	7.1			
	7.5			
	10.5			

^a All spectra obtained at 100 MHz. Positions of most hydrogens bonded to boron were determined by decoupling boron. ^b Solvents included CD $_3$ CN and CD $_2$ Cl $_2$ unless otherwise indicated. ^c In most cases poorly resolved coupling to a single ^{11}B was detected with $J \approx 70$ Hz. ^d The center of each resonance type is shown. Fine structure was observed in all cases and was similar to that observed in the free ion or molecule.

evident until either three CO molecules or a single CO and a THF molecule have been removed, suggesting that the hydrogens are more strongly bound to the borane ligand than the carbonyl groups are bound to the manganese.

The bonding electron bookkeeping for these metalloborane complexes can be viewed in several ways. Perhaps the simplest approach is to consider that the metals are formally Mn(I) and Re(I)¹⁰ and that the tridentate borane ligands are therefore B $_9$ H $_{13}^{2-}$ and B $_9$ H $_{12}L^-$ (L = Lewis base) anions,

which are related to one another by the formal exchange of hydride, H^- , in I and VI and the ether ligand L in II, III, and IV. That this is a reasonable analogy has been demonstrated by the oxidation of I in the presence of THF to produce II (eq 2). In order for Mn and Re to obey the EAN rule, the B_9 ligand must contribute a total of six electrons to the metal.

Experimental Section

Potassium tetradecahydroonaborate(1-), KB_9H_{14} , was made by a modification of the method of Benjamin, Stafiej, and Takacs.¹¹ After the synthesis of $B_9H_{14}^-$ by acidification of the previously basic reaction mixture,¹¹ the solution was cooled in an ice bath and solid potassium carbonate was slowly added (with stirring) until a copious precipitate was observed. The solid was collected and partly dried by evacuation at room temperature. The KB_9H_{14} was extracted from the excess potassium carbonate using diethyl ether. The ether solution was dried and the ether removed by evaporation under vacuum. Manganese and rhenium pentacarbonyl bromides were prepared from the parent metal pentacarbonyl dimer, $M_2(CO)_{10}$, and bromine. Tetrahydrofuran (THF) was distilled from lithium aluminum hydride (usually directly into the reaction flask) and 1,2-dimethoxyethane (glyme) was distilled from sodium naphthalenide. All other reagents and solvents were reagent grade and were used as received.

$[Me_4N][6-(CO)_3-6-MnB_9H_{13}]$, I, and 2-THF-6-(CO)₃-6-MnB₉H₁₂, II. In a typical reaction 1.466 g (9.74 mmol) of KB_9H_{14} and 2.846 g (10.37 mmol) of $Mn(CO)_5Br$ were placed in a nitrogen-flushed reaction flask, charged with freshly distilled dry THF, and heated to reflux in a nitrogen atmosphere for 1.5 hr. The solvent was removed by distillation under vacuum until only a dark red oil remained. Water was added to displace residual THF, which was then removed by evaporation at room temperature using a water aspirator. The water slurry remaining was filtered, and the red solution was treated with excess tetramethylammonium chloride to produce an orange precipitate, I, which was subsequently recrystallized from dichloromethane and heptane.

The brown-red precipitate from the original suspension was then extracted with hot heptane. Upon slow cooling of the filtered heptane extract dark red sublimable crystals of II formed.

The yield of I was 1.392 g (4.29 mmol), or 44%, and that of II was 0.078 g (0.244 mmol), or 2.5%. The yields varied from 30 to 50% for I and up to 5% for II. It was found that as the reflux time increased, the amount of II increased up to about 6–10 hr, after which the yield decreased with reflux time.

An alternate method for separation involved the use of liquid chromatography on a Florisil solid phase. Elution of II was achieved using a mixture of heptane and up to 25% dichloromethane. A black crystalline product, as yet uncharacterized, was eluted using a 1:1 dichloromethane–heptane mixture. An unstable green material was next eluted using pure dichloromethane and I was eluted with tetrahydrofuran.

$[Me_4N][6-(CO)_3-6-MnB_9H_{13}]$, I. *Anal.* Calcd: C, 25.97; H, 7.79; B, 30.08; Mn, 16.99; N, 4.33. Found: C, 23.21; H, 7.93; B, 30.65; Mn, 17.18; N, 4.37.

One to one electrolyte behavior of I in CH_3CN is indicated by its molar conductance of $148 \text{ cm}^2 \text{ ohm}^{-1} \text{ mol}^{-1}$ compared to a value of $126 \text{ cm}^2 \text{ ohm}^{-1} \text{ mol}^{-1}$ obtained for tetraethylammonium picrate under the same conditions. Visible and uv spectral maxima (CH_2Cl_2): $460 \mu\text{m}$ (ϵ 440), $312 \mu\text{m}$ (ϵ 2440). Other characterization data are in Tables IV–VI.

2-THF-6-(CO)₃-6-MnB₉H₁₂, II. The molecular structure of II was determined via X-ray crystallography by Schaeffer, *et al.*⁴ The mass spectrum of II shows envelopes of peaks corresponding to the parent ions and to ions formed by loss of two and three carbonyl groups. Following these is an envelope corresponding to the loss of a tetrahydrofuran molecule and one carbonyl group and a series of envelopes characteristic of boron hydrides.

The exact *m/e* values were determined for a parent ion and an ion corresponding to the parent minus two carbonyl groups: calcd for $^{55}Mn(^{12}C^{16}O)_3^{11}B_9H_{12}^+$, 322.1580; found, 322.1603; calcd for $^{55}Mn^{12}C^{16}O^{11}B_9H_{12}^+$, 266.1682; found, 266.1684. Visible–uv spectral maxima (CH_2Cl_2): $456 \mu\text{m}$ (ϵ 375), $308 \mu\text{m}$ (ϵ 2330).

(10) We previously regarded the B_9 ligands as five-electron donors to the metals which were assigned a formal oxidation state of zero.⁴ The assignment of a +1 formal oxidation state to the metals now appears to be more consistent with the overall behavior patterns of these metalloboranes.

(11) L. E. Benjamin, S. F. Stafiej, and E. A. Takacs, *J. Amer. Chem. Soc.*, **85**, 2674 (1963).

Table VI. Infrared Spectral Data^a

I, $[Me_4N][6-(CO)_3-6-MnB_9H_{13}]$	2630 m, 2560 s, 2480 s, 2025 vs, sh, 2060 s, sh, 2005 vs, sh, 1485 m, 1420 w, 1095 m, 1020 m, 945 m, 930 w, 885 w, 845 w, 815 w, 785 s, 725 w, 715 w, 665 s
II, 2-THF-6-(CO) ₃ -6-MnB ₉ H ₁₂	3850 m, b, 2610 s, 2580 s, 2520 s, 2055 vs, sh, 1950 vs, sh, 1930 vs, 1505 w, b, 1430 w, b, 1360 m, sh, 1260 w, 1190 w, 1150 vw, 1100 w, 1060 w, 1025 m, 1010 m, s, 970 s, 955 m, s, 930 m, s, 860 m, 810 m, 780 w, 765 w, 735 m, 680 m, s
III, 5-THF-6-(CO) ₃ -6-MnB ₉ H ₁₂	3440 m, b, 3260 m, 3010 w, sh, 2980 w, sh, 2595 s, 2525 s, sh, 2055 vvs, 1960 vvs, 1925 vs, sh, 1730 m, 1470 m, b, 1270 w, 1210 w, 1110 w, 1050 m, 1015 m, 980 m, 940 m, sh, 870 w, sh, 860 w, 840 w, 810 w, 710 m, sh, 690 m, 670 m, 650 m
IV, 2-(OEt ₂)-6-(CO) ₃ -6-MnB ₉ H ₁₂	3040 w, 2660 s, sh, 2610 s, sh, 2550 vs, 2060 vvs, 1945 vvs, b, 1570 w, 1555 w, 1520 w, 1480 w, b, 1445 w, 1400 m, 1335 w, 1300 w, 1205 m, 1160 w, 1100 m, 1030 s, sh, 1020 s, 1000 s, sh, 970 w, 945 m, 915 m, 895 m, 860 s, 820 s, 805 m, sh, 780 s, 730 s, 680 m
V, $[Me_4N][6-(CO)_3-6-MnB_9H_{13}]$	3450 m, b, 2530 s, 2130 w, 2030 s, sh, 1950 s, sh, 1905 s, sh, 1880 s, sh, 1485 s, 1175 w, 1105 w, 1085 w, 1020 m, 950 m, 780 w, 700 m, b

^a All spectra listed were observed as KBr mulls and are in $\text{cm}^{-1} \pm 10 \text{ cm}^{-1}$.

Other characterization data are in Tables IV–VI.

Oxidation of I to II. A 0.9367-g (2.9-mmol) sample of I was allowed to stir at room temperature for several days in a tetrahydrofuran solution containing 0.1 g of iodine (8 mmol). Chromatographic separation, as previously described, resulted in isolation of 0.1426 g of II, a yield of 15.2%. A similar experiment conducted in refluxing tetrahydrofuran for 1 hr resulted in a 10.6% yield. Alternately a tetrahydrofuran solution of 2.0515 g (6.4 mmol) of I and 1.7341 g (6.35 mmol) of $HgCl_2$ was stirred for 0.5 hr at ambient temperature. A gray flocculent precipitate containing some elemental mercury formed almost immediately. After evaporation of the THF, 0.546 g (26%) of II was extracted from the reaction mixture using hot heptane.

5-THF-6-(CO)₃-6-MnB₉H₁₂, III. A 3.869-g (13.3-mmol) sample of $Mn(CO)_5Br$ was allowed to react with 0.996 g (6.62 mmol) of KB_9H_{14} in refluxing THF for 2 hr. The solvent was then removed and evaporated under vacuum, and a minimum of dichloromethane was added to dissolve the remaining reaction mixture. This solution was chromatographed on Florisil. Fractions found to contain infrared BH stretching bands were eluted with 30% dichloromethane in heptane and 40–60% dichloromethane in heptane and tetrahydrofuran. The first and third fractions proved to be II and I, respectively. The second band, III, had an infrared spectrum different from that of any previously isolated complex. Yields were as follows: the tetramethylammonium salt of I, 0.3226 g (1.0 mmol), 15%; II, 0.1482 g (0.46 mmol), 6.9%; III, 0.1554 g (0.48 mmol), 7.2%.

The mass spectrum of III was similar to that of II. Visible–uv spectral maxima (CH_2Cl_2): $585 \mu\text{m}$ (ϵ 90), $483 \mu\text{m}$ (ϵ 1200), $313 \mu\text{m}$ (ϵ 5040), $225 \mu\text{m}$ (ϵ 12,100). Other characterization data are in Tables IV–VI.

In a similar reaction using diethyl ether as the solvent the only product isolated was I.

Crystal Data and Structure Determination of III. Suitable red crystals of III for X-ray analysis were obtained from the slow evaporation of a chloroform–carbon tetrachloride solution. A crystal of III with approximate dimensions of 32 mm × 25 mm × 16 mm,

Table VII. Coordinates^a and Anisotropic Thermal Parameters^b for All Nonhydrogen Atoms in 5-THF-6-(CO)₃-6-MnB₉H₁₂, III

	<i>x</i>	<i>y</i>	<i>z</i>	10 ⁴ β ₁₁	10 ⁴ β ₂₂	10 ⁴ β ₃₃	10 ⁴ β ₁₂	10 ⁴ β ₁₃	10 ⁴ β ₂₃
Mn	0.28742 (7)	0.13053 (5)	0.37249 (9)	106 (6)	46 (4)	181 (8)	23 (4)	44 (6)	11 (5)
C(1)	0.1316 (5)	0.1757 (4)	0.3440 (7)	134 (15)	74 (12)	307 (23)	23 (13)	95 (18)	24 (15)
O(1)	0.0360 (4)	0.2077 (3)	0.3364 (6)	167 (12)	136 (11)	593 (24)	83 (12)	160 (17)	49 (16)
C(2)	0.2486 (5)	0.0756 (3)	0.5965 (7)	178 (16)	57 (11)	291 (23)	27 (13)	96 (18)	7 (15)
O(2)	0.2223 (5)	0.0441 (3)	0.7415 (5)	342 (16)	101 (11)	302 (20)	52 (13)	194 (18)	62 (14)
C(3)	0.1737 (5)	0.0045 (3)	0.2187 (6)	142 (15)	64 (11)	239 (22)	30 (13)	55 (17)	33 (15)
O(3)	0.1033 (4)	-0.0748 (2)	0.1206 (5)	213 (15)	64 (10)	334 (20)	4 (11)	24 (16)	-21 (13)
B(1)	0.5777 (5)	0.3620 (4)	0.3411 (7)	96 (15)	52 (11)	183 (22)	21 (12)	19 (17)	11 (15)
B(2)	0.4661 (5)	0.2893 (3)	0.4941 (6)	93 (14)	49 (11)	157 (21)	23 (12)	40 (16)	3 (14)
B(3)	0.6569 (5)	0.3011 (4)	0.5431 (7)	98 (15)	73 (12)	162 (22)	35 (13)	-1 (16)	2 (15)
B(4)	0.7302 (5)	0.3210 (4)	0.3269 (8)	91 (15)	90 (13)	280 (24)	42 (14)	52 (18)	43 (17)
B(5)	0.3960 (5)	0.2755 (3)	0.2316 (6)	85 (14)	48 (11)	164 (21)	27 (12)	17 (16)	9 (14)
B(7)	0.5217 (6)	0.1747 (4)	0.5538 (7)	132 (15)	64 (12)	184 (22)	44 (13)	41 (17)	21 (15)
B(8)	0.7010 (6)	0.1988 (4)	0.4394 (7)	127 (15)	89 (13)	197 (23)	60 (14)	16 (18)	13 (16)
B(9)	0.6673 (6)	0.2025 (5)	0.1768 (8)	152 (15)	118 (14)	208 (23)	84 (15)	73 (18)	25 (17)
B(10)	0.5700 (5)	0.2939 (4)	0.1188 (7)	105 (15)	81 (12)	201 (22)	43 (13)	58 (17)	34 (16)
O(4)	0.2952 (3)	0.3320 (2)	0.1180 (4)	123 (11)	54 (8)	196 (17)	43 (10)	-6 (13)	-2 (11)
C(4)	0.2052 (5)	0.2964 (4)	-0.0916 (6)	121 (15)	90 (12)	214 (22)	39 (13)	19 (17)	33 (15)
C(5)	0.1214 (7)	0.3709 (5)	-0.1395 (8)	241 (18)	127 (14)	343 (27)	104 (17)	-65 (21)	1 (19)
C(6)	0.1381 (6)	0.4333 (5)	0.0495 (9)	201 (17)	132 (14)	451 (28)	103 (16)	64 (20)	66 (19)
C(7)	0.2794 (6)	0.4301 (4)	0.1974 (8)	209 (16)	91 (12)	381 (26)	90 (15)	28 (19)	12 (17)

^a The estimated standard deviation in the last digit is given in parentheses. ^b Anisotropic temperature factors are of the form $\exp[-(\beta_{11}h^2 + \beta_{22}k^2 + \beta_{33}l^2 + 2\beta_{12}hk + 2\beta_{13}hl + 2\beta_{23}kl)]$.

bounded by the (-101), (021), (160), (001), and ±[(1-10), (010)] faces, was mounted on a Syntex P1 autodiffractometer equipped with Mo Kα radiation. After careful centering of the crystal using optical and X-ray tube alignment, 15 preliminary reflections were centered in 2θ, χ, and ω. The correct indices were automatically assigned and were used in a least-squares procedure to give lattice and orientation parameters.¹² The cell parameters measured corresponded to a triclinic unit cell with dimensions *a* = 9.828 (3) Å, *b* = 13.305 (5) Å, and *c* = 6.937 (2) Å, α = 90.81 (27)°, β = 104.23 (2)°, γ = 109.7 (3)°, and *V* = 822.1 (5) Å³ (estimated standard deviation in parentheses). A density measurement by the flotation method verified the molecular formula: calcd for two molecules per unit cell, 1.305 g cm⁻³; found, 1.315 g cm⁻³.

A total of 2390 reflections were measured with the usual θ-2θ scan technique (2θ varied from 3.0 to 45°) and corrected for Lorentz-polarization effects. Of the 2172 independent reflections, 1803 were observed (*I* > 2σ(*I*)) and were used throughout the structural analysis. The standard deviation of each corrected intensity was estimated from the formula $\sigma(I) = T_R S + (B_1 + B_2)/B_R + qI^{1/2}$, where *T_R* is the 2θ scan rate in degrees per minute, *S* is the total integrated scan count, *B₁* and *B₂* are the background counts, and *B_R* is the ratio of the background to scan count times. *q* was assigned a value of 0.003. The integrated intensity, *I*, was taken as $[S - (B_1 + B_2)/B_R] T_R$. The two standard reflections, which were used to monitor the intensity for electronic and crystal stability every 50 reflections, indicated no significant decay, and no normalization was needed. The effects of absorption ($\mu = 8.45 \text{ cm}^{-1}$) were ignored as the variation in absorption between the maximum and minimum test reflections for the blocklike crystal was 2.8% on *F*.

The solution of the structure proceeded *via* standard heavy-atom methods. The Patterson function was easily interpreted¹³ in terms of one heavy atom per molecule, assuming the centric space group P1. The first Fourier synthesis¹⁴ phased on the coordinates of the Mn (*R*₁ = 34.3%) yielded the structure directly (*R*₁ = 19.7%).¹⁵

After several preliminary cycles of full-matrix least squares¹⁶ on all nonhydrogen atoms allowing isotropic variation of thermal parameters, the *R*₁ and *R*₂ values were reduced to 9.3 and 12.2%, respectively. A difference map then revealed the positions of all but two hydrogens and these (β_{iso} for hydrogen is 3.5 Å²) were then used in three full-matrix least-squares anisotropic cycles to give *R*₁ =

Table VIII. Hydrogen Coordinates^a for 5-THF-6-(CO)₃-6-MnB₉H₁₂, III

	<i>x</i>	<i>y</i>	<i>z</i>
H(1)	0.7393	0.3438	0.7009
H(2)	0.4341	0.3351	0.5981
H(3)	0.5975	0.4497	0.3321
H(4)	0.8281	0.3830	0.3214
H(5)	0.3417	0.1849	0.1759
H(6)	0.4528	0.0910	0.4310
H(7)	0.5458	0.1432	0.7130
H(8)	0.5750	0.3294	-0.0262
H(9)	0.7200	0.1688	0.0782
H(10)	0.7975	0.1771	0.5379
H(11)	0.6288	0.1399	0.2906
H(12)	0.5287	0.2007	0.0792
H(13)	0.1390	0.2378	-0.0667
H(14)	0.2721	0.3090	-0.1583
H(15)	0.0000	0.3417	-0.2738
H(16)	0.1841	0.3914	-0.2088
H(17)	0.0775	0.3954	0.1167
H(18)	0.1825	0.4638	-0.0125
H(19)	0.3295	0.4580	0.1359
H(20)	0.2495	0.4070	0.3017

^a Hydrogen positions were found using a three-dimensional Fourier difference map and were not allowed to vary.

5.0 and *R*₂ = 6.3%. Another difference map gave the coordinates of the two remaining hydrogens. Two more cycles of full-matrix least squares reduced *R*₁ and *R*₂ to 4.5 and 5.5%, respectively. At no time were the hydrogen parameters allowed to vary.

All least-squares refinements were based on the minimization of $\sum w_i(|F_o| - |F_c|)^2$. The atomic scattering factors used for all nonhydrogen atoms were those compiled by Hanson, *et al.*¹⁷

The positions and thermal parameters for all nonhydrogen atoms are given in Table VII; hydrogen positions are listed in Table VIII. Interatomic distances and bond angles with estimated standard deviations, calculated using the Busing-Martin-Levy function and error program¹⁸ from the full inverse matrix, are presented in Tables I and II.¹⁹

2-Et, O-6-(CO)₃-6-MnB₉H₁₂, IV. In a typical reaction, a solution of 9.931 g of KB₉H₁₄ (6.2 mmol) and 1.436 g of Mn(CO)₅Br

(12) "P1 Autodiffractometer Operations Manual," Syntex Analytical Instruments Division, Cupertino, Calif., 1970.

(13) J. C. Calabrese, Ph.D. Thesis (Appendix), University of Wisconsin, Madison, Wis., 1971.

(14) J. C. Calabrese, "A Three-Dimensional Crystallographic Fourier Summation Program," University of Wisconsin, Madison, Wis., 1973.

(15) $R_1 = \sum |F_o| - |F_c| / \sum |F_o|$ and $R_2 = [\sum w_i |F_o| - |F_c|^2 / \sum w_i |F_o|^2]^{1/2}$.

(16) W. R. Busing, K. O. Martin, and H. A. Levy, "ORFLS, a Fortran Crystallographic Least Squares Program," Report ORNL-TM-305, Oak Ridge National Laboratory, Oak Ridge, Tenn., 1962.

(17) H. P. Hanson, F. Herman, J. D. Lea, and S. Skillman, *Acta Crystallogr.*, 17, 1040 (1964). Anomalous dispersion corrections were made using values from the "International Tables for X-Ray Crystallography," Vol. III, K. Lonsdale, Ed., Kynoch Press, Birmingham, England, 1962.

(18) W. R. Busing, K. O. Martin, and H. A. Levy, "ORFFE, a Fortran Crystallographic Function and Error Program," Report ORNL-TM-306, Oak Ridge National Laboratory, Oak Ridge, Tenn., 1964.

(19) See paragraph at end of paper regarding supplementary material.

(5.2 mmol) was refluxed in diethyl ether for 3–6 hr. The reaction mixture was then stripped of solvent by evaporation under vacuum, and the remaining oily red material was dissolved in a minimum of dichloromethane and chromatographed on Florisil. Elution with heptane gave a bright yellow band containing $(\text{CO})_3\text{MnB}_9\text{H}_{13}$, which, if allowed to stand for several hours, showed very definite signs of decomposition.

A second band was eluted using dichloromethane, after preliminary experiments showed that mixtures of heptane and dichloromethane produced no further separations. Evaporation of the solvent and recrystallization from hot heptane produced reddish orange crystals of IV. Tetrahydrofuran removed the final product, which was isolated and identified as I. In addition, a brownish band was often left which could be eluted with acetone. However, this material was very unstable and no attempt was made to characterize it. Yields for a typical reaction were as follows: I, 0.2699 g (0.836 mmol), 15.9%; IV, 0.0106 g (0.03 mmol), 0.63%.

The mass spectrum for IV, 2-Et, O-6-Mn(CO)₃B₉H₁₂, was quite similar to that for 2-THF-6-Mn(CO)₃B₉H₁₂. Mass envelopes were again observed at values corresponding to parent mass, P, P-2(CO), P-3(CO), and P-(Et₂O + CO). Below this value, envelopes characteristic of boron hydride fragmentation patterns were present. Exact *m/e* determination verified the identity of a parent fragment: calcd for ⁵⁵Mn(¹²C¹⁶O)₃¹¹B₉¹H₁₂·¹⁶O(¹²C₂¹H₂)₂, 324.1737; found, 324.1772. Other characterization data are in Tables IV–VI and Figure 5.

[Me₂N]⁺[6-(CO)₃-6-ReB₉H₁₂]⁻, V. The white Re(CO)₅Br, 1.960 g (4.83 mmol), was allowed to react in refluxing tetrahydrofuran with 0.995 g (6.62 mmol) of KB₉H₁₄ for 3–6 hr. The solvent was evaporated and the residue chromatographed on Florisil. Two

yellow materials were eluted using dichloromethane and THF. The covalent 2-THF-6-(CO)₃-6-ReB₉H₁₂ was assumed to be the species eluted by dichloromethane. This material was extremely air and water sensitive, however, and has not been fully characterized. The THF eluent contained the 6-(CO)₃-6-ReB₉H₁₃⁻ anion which was isolated as the tetramethylammonium salt in a yield of 1.0321 g (2.27 mmol), 47%. Characterization data are in Tables IV–VI.

Acknowledgments. The authors are indebted to A. O. Clouse and the Indiana University Chemistry Department for the 70.6-MHz ¹¹B nmr spectral measurements and to Dr. J. C. Calabrese for assistance with the X-ray analysis. This work was supported in part by grants from the Office of Naval Research and the National Science Foundation.

Registry No. I, 41729-34-4; II, 51801-39-9; III, 51801-38-8; IV, 51801-37-7; V, 51801-36-6; KB₉H₁₄, 39296-28-1; Mn(CO)₅Br, 14516-54-2; Re(CO)₅Br, 14220-21-4; ¹¹B, 14798-13-1.

Supplementary Material Available. A listing of structure factor amplitudes will appear following these pages in the microfilm edition of this volume of the journal. Photocopies of the supplementary material from this paper only or microfiche (105 × 148 mm, 24 × reduction, negatives) containing all of the supplementary material for the papers in this issue may be obtained from the Journals Department, American Chemical Society, 1155 16th St., N.W., Washington, D. C. 20036. Remit check or money order for \$4.00 for photocopy or \$2.00 for microfiche, referring to code number INORG-74-2261.

Contribution from the Departments of Chemistry, the University of Michigan, Ann Arbor, Michigan 48104, and the University of Utah, Salt Lake City, Utah 84112

Preparation and Structure of Trifluorophosphine-Trichloroalane and a Study of Related Acid-Base Systems

E. R. ALTON, R. G. MONTEMAYOR, and R. W. PARRY*

Received February 27, 1974

AIC40131N

Aluminum chloride reacts with an excess of trifluorophosphine under pressure to give a compound of formula F₃P·AlCl₃. Molecular weight and nmr data support an ethane-like structure involving a P–Al bond. The compound undergoes halogen exchange to give PCl₃ and AlF₃. Evidence for interaction of Al₂(CH₃)₆ with both PF₃ and NH₃ was found, but all attempts to bring about reaction between Al₂(CH₃)₆ and CO were unsuccessful. No reaction could be detected between CO and Al₂Cl₆, or between PF₃ and BF₃. About 2.5 mole % of Al₂Cl₆ will dissolve in excess PCl₃ at 130°, but the solid precipitates out almost completely when the temperature is lowered to 25°. In agreement with observations of Holmes, we find no evidence for compound formation between PCl₃ and AlCl₃.

The reaction between PF₃ and B₂H₆ gives the well-known compound F₃P·BH₃ even though inductive effect arguments suggest that PF₃ should not be a significant Lewis base.¹ Theoretical hyperconjugation type arguments² which were advanced to explain the stability of F₃PBH₃ suggested that a study of the system F₃P–Al₂Cl₆ would be of interest. Such a study, completed in this laboratory, has resulted in the preparation and characterization of the compound F₃P·AlCl₃ as a monomeric, presumably ethane-like structure with a P–Al bond. Inasmuch as recent work³ has shown that [(CH₃)₂N]₂PCl reacts with AlCl₃ to give an ionic species containing the AlCl₄⁻ anion, the ethane-like structure here is significant.

* To whom correspondence should be addressed at The University of Utah.

(1) R. W. Parry and T. C. Bissot, Jr., *J. Amer. Chem. Soc.*, **78**, 1524 (1956).

(2) S. Ahrland, J. Chatt, and N. R. Davies, *Quart. Rev., Chem. Soc.*, **12**, 266 (1958).

(3) M. G. Thomas, R. L. Kopp, C. W. Schultz, and R. W. Parry, submitted for publication in *J. Amer. Chem. Soc.*

The System Aluminum Chloride-Phosphorus Trifluoride

Freshly prepared, scrupulously dry aluminum chloride reacts with phosphorus trifluoride at 8 atm pressure in a sealed glass bomb. At room temperature and the conditions used in this study the reaction was essentially quantitative after 4 hr (Table I). Shorter periods of time or lower pressures usually produced incomplete reaction. Longer periods of time or certain still incompletely defined impurities promoted a halide shift. The overall equation is

$$\text{F}_3\text{P}(\text{g}) + \text{Al}_2\text{Cl}_6(\text{s}) \rightarrow \text{F}_3\text{P}\cdot\text{AlCl}_3(\text{s}) \rightarrow \text{AlF}_3(\text{s}) + \text{PCl}_3(\text{l})$$

The halide shift occurs spontaneously and fairly rapidly above –20° when the large excess of PF₃ is removed. Excess PF₃ above the solid seems to have an inhibitory effect on halogen transfer. One of the most reasonable possibilities for an intermediate in the halogen-transfer process would involve possible P–F–Al and P–Cl–Al bridge structures in which the aluminum assumes coordination numbers of 5 or 6 in the activated complex.⁴ If this model is assumed, the